



## Beyond the acceptance limit of DRAGON: The case of the ${}^6\text{Li}(\alpha, \gamma){}^{10}\text{B}$ reaction

A. Psaltis<sup>a,\*</sup>, A.A. Chen<sup>a</sup>, D.S. Connolly<sup>b</sup>, B. Davids<sup>b</sup>, G. Gilardy<sup>c,d</sup>, R. Giri<sup>h</sup>, U. Greife<sup>e</sup>,  
W. Huang<sup>b,f</sup>, D.A. Hutcheon<sup>b</sup>, J. Karpesky<sup>e</sup>, A. Lennarz<sup>b</sup>, J. Liang<sup>a</sup>, M. Lovely<sup>e</sup>, S.N. Paneru<sup>h</sup>,  
C. Ruiz<sup>b</sup>, G. Tenkila<sup>g</sup>, M. Williams<sup>b,i</sup>

<sup>a</sup> Department of Physics and Astronomy, McMaster University, Hamilton, Ontario L8S 4M1, Canada

<sup>b</sup> TRIUMF, 4004 Wesbrook Mall, Vancouver, British Columbia V6T 2A3, Canada

<sup>c</sup> Department of Physics, Joint Institute for Nuclear Astrophysics, University of Notre Dame, Notre Dame, IN 46556, USA

<sup>d</sup> Centre d'Études Nucléaires de Bordeaux Gradignan, UMR 5797 CNRS/IN2P3 - Université de Bordeaux, 19 Chemin du Solarium, CS 10120, F-33175 Gradignan, France

<sup>e</sup> Department of Physics, Colorado School of Mines, Golden, CO 80401, USA

<sup>f</sup> Physics Department, University of Northern British Columbia, Prince George, BC V2N 4Z9, Canada

<sup>g</sup> Department of Physics and Astronomy, University of British Columbia, Vancouver, British Columbia V6T 1Z4, Canada

<sup>h</sup> Department of Physics, and Astronomy, Ohio University, Athens, OH 45701, USA

<sup>i</sup> Department of Physics, University of York, Heslington, York YO10 5DD, United Kingdom

### ARTICLE INFO

#### Keywords:

Recoil separators  
Inverse kinematics  
Radiative capture  
Resonance strength

### ABSTRACT

Radiative capture reactions play a pivotal role for our understanding of the origin of the elements in the cosmos. Recoil separators provide an effective way to study these reactions, in inverse kinematics, and take advantage of the use of radioactive ion beams. However, a limiting factor in the study of radiative capture reactions in inverse kinematics is the momentum spread of the product nuclei, which can result in an angular spread larger than the geometric acceptance of the separator. The DRAGON facility at TRIUMF is a versatile recoil separator, designed to study radiative capture reactions relevant to astrophysics in the  $A \sim 10\text{--}30$  region. In this work we present the first attempt to study with DRAGON a reaction,  ${}^6\text{Li}(\alpha, \gamma){}^{10}\text{B}$ , for which the recoil angular spread exceeds DRAGON's acceptance. Our result is in good agreement with the literature value, showing that DRAGON can measure resonance strengths of astrophysically important reactions even when not all the recoils enter the separator.

### 1. Introduction

Radiative capture reactions involving hydrogen and helium are of pivotal importance for nuclear astrophysics. Knowing their cross sections improves reaction network calculations and thus our predictions for the origin of the elements in the universe. Given that these reactions involve the two most abundant elements in the cosmos, they occur in almost any astrophysical scenario, including quiescent (e.g. Ne–Na, Mg–Al cycles) and explosive (e.g.  $rp$ -process,  $\nu p$ -process) stellar burning. These reactions are traditionally studied using intense proton and  $\alpha$ -beams from low-energy accelerators, impinging onto a heavy target. This technique, even though it is still used until today with great success, has some drawbacks, such as the beam induced background and the inability to use short-lived targets. Using recoil separators, radiative capture reactions can be studied in inverse kinematics, with a heavy ion beam (stable or radioactive) impinging on a gas target (usually hydrogen or helium). Their advent remedies the aforementioned problems, but imposed some new ones, mainly of a geometric nature [1,2].

The Detector of Recoils and Gammas of Nuclear reactions (DRAGON) facility in the Isotope Separator and Accelerator-I (ISAC-I) experimental hall at TRIUMF, Canada's particle accelerator center in Vancouver, BC has carried out many of the radiative capture measurements involving radioactive ion beams to date. Even though it was constructed to study reactions with beams up to  $A = 30$  [3,4], over the last two decades, DRAGON has demonstrated versatility, having performed experiments from  $A = 3$ , e.g.,  ${}^3\text{He}(\alpha, \gamma){}^7\text{Be}$  [5], to  $A = 76$ , e.g.,  ${}^{76}\text{Se}(\alpha, \gamma){}^{80}\text{Kr}$  [6].

The experiment presented in this work is a proof of the capability of DRAGON to measure resonant cross sections of radiative capture reactions of astrophysical interest in which the angular cone of the recoils exceeds its geometric acceptance. It was selected as a benchmark for the measurement of unknown resonance strengths of the  ${}^7\text{Be}(\alpha, \gamma){}^{11}\text{C}$  reaction, which is important for  $\nu p$ -process nucleosynthesis (see Table 1). In the past, there have been acceptance-challenging experiments for nuclear reaction studies with DRAGON, such as the  ${}^{12}\text{C}({}^{16}\text{O}, \gamma){}^{28}\text{Si}$

\* Corresponding author.

E-mail address: [psaltisa@mcmaster.ca](mailto:psaltisa@mcmaster.ca) (A. Psaltis).

**Table 1**

List of some astrophysically important reactions in the  $A = 7-24$  mass region. The  $Q$ -value of each reaction is presented in MeV, along with the astrophysical scenario that it affects and the respective energy region of the Gamow window in the center of mass system ( $E_{cm}$ ). The  $\theta_{r,max}$  value for each reaction is the maximum angle the recoils can have in the Gamow window listed in the second column. The reactions marked with  $\star$  have been measured using the DRAGON recoil separator, but not necessarily in the Gamow window, and the reactions marked with  $\dagger$  have an angular cone greater than DRAGON's maximum acceptance  $\theta_{DRAGON} = \pm 21$  mrad. See text for details.

Reaction	Q value (MeV) $E_{cm}$ (MeV)	Astrophysical Scenario (nucleosynthesis process)	$\theta_{r,max}$ (mrad)
${}^7\text{Li}(\alpha, \gamma){}^{11}\text{B}^\dagger$	8.664 0.7–3.6	Core-Collapse Supernovae $\nu$ -process	$\pm 51$
${}^7\text{Be}(\alpha, \gamma){}^{11}\text{C}^\dagger$	7.544 0.5–1.2	Core-Collapse Supernovae $\nu p$ -process	$\pm 44$
${}^7\text{Be}(p, \gamma){}^8\text{B}$	0.136 0.02	Sun $pp$ -chains (solar $\nu$ )	$\pm 3$
${}^{12}\text{C}(\alpha, \gamma){}^{16}\text{O}^{\dagger\star}$	7.162 0.03	Intermediate mass/Massive stars Quiescent helium burning	$\pm 138$
${}^{13}\text{N}(p, \gamma){}^{14}\text{O}$	4.626 0.3–2.2	X-ray bursts hot CNO cycle	$\pm 15$
${}^{15}\text{O}(\alpha, \gamma){}^{19}\text{Ne}$	3.528 1.5–4.6	X-ray bursts hot-CNO cycle	$\pm 21$
${}^{16}\text{O}(\alpha, \gamma){}^{20}\text{Ne}^{\dagger\star}$	4.730 0.02	Intermediate mass/Massive stars Quiescent helium burning	$\pm 87$
${}^{17}\text{O}(\alpha, \gamma){}^{18}\text{F}^\dagger$	7.348 0.1–0.5	AGB stars, massive stars, and novae $s$ -process	$\pm 64$
${}^{18}\text{O}(\alpha, \gamma){}^{22}\text{Ne}^\dagger$	9.667 0.6–2.3	Intermediate mass/Massive stars $s$ -process	$\pm 55$
${}^{20}\text{Ne}(\alpha, \gamma){}^{24}\text{Mg}$	9.316 0.04	Intermediate mass/Massive stars Quiescent helium burning	$\pm 105$
${}^{22}\text{Ne}(p, \gamma){}^{23}\text{Na}^\star$	8.794 0.3–0.5	AGB stars/ classical novae Ne–Na cycle	$\pm 18$
${}^{22}\text{Ne}(\alpha, \gamma){}^{26}\text{Mg}^\dagger$	10.614 0.038–1.450	Intermediate mass/Massive stars $s$ -process	$\pm 105$
${}^{23}\text{Mg}(p, \gamma){}^{24}\text{Al}^\star$	1.863 0.5–0.9	O–Ne–Mg novae Ne–Na cycle	$\pm 3$

and  ${}^{12}\text{C}(\alpha, \gamma){}^{16}\text{O}$ , reported in Refs. [7,8], but these studies did not involve the measurement of a resonance strength. For this test we used a known resonance at a center of mass energy of  $E_r = 1458.5(6)$  keV of the  ${}^6\text{Li}(\alpha, \gamma){}^{10}\text{B}$  reaction whose strength was originally measured by Forsyth et al. in forward kinematics [9]. The present measurement was performed in inverse kinematics, using a stable  ${}^6\text{Li}$  beam provided by the TRIUMF Off-Line Ion Source (OLIS) [10].

The paper is structured as follows: in Section 2 we give a brief overview of conducting experiments using recoil separators and the challenges of studying reactions with low mass ion beams. In Section 3 we discuss the measurement by Forsyth et al. In Section 4 we give an overview of DRAGON and the experimental setup, in Section 5 we present the data analysis and the results, and finally in Section 6 we present our conclusions by discussing the final results in more detail.

## 2. Radiative capture reactions using recoil separators

Radiative capture reactions in inverse kinematics occur in a usually gaseous target, at rest in the laboratory frame, with the entire laboratory momentum being carried by the beam. The compound nucleus is formed in an excited state with energy

$$E_x = E_{cm} + Q \quad (1)$$

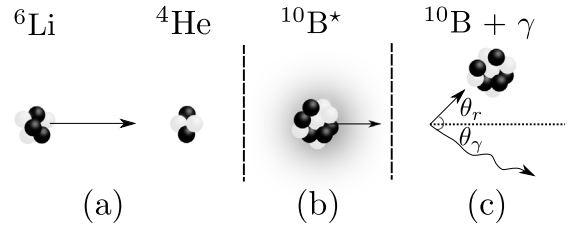


**Fig. 1.** Schematic representation of a radiative  $\alpha$ -capture on  ${}^6\text{Li}$  in inverse kinematics: (a) beam ( ${}^6\text{Li}$ ) and target ( ${}^4\text{He}$ ) particles interact, (b) the compound nucleus ( ${}^{10}\text{B}$ ) is synthesized in an excited state and then, (c) it decays by emitting a  $\gamma$  ray. The recoil nucleus and the  $\gamma$  ray are emitted in angles  $\theta_r$  and  $\theta_\gamma$  in the lab system respectively. See the text for details.

where  $E_{cm}$  is the energy in the center of mass system, and when the reaction proceeds through a resonance,  $E_{cm} = E_r$ .  $Q = (m_1 + m_2 - m_3)c^2$  is the reaction  $Q$  value, where  $m_1, m_2$  and  $m_3$  are the masses of the projectile, the target, and the recoil, respectively.

The excited nucleus decays by emitting one or multiple  $\gamma$  rays ( $\sum_i E_{\gamma_i} = E_x$ ), which carry some of the initial momentum, and thus the products (recoil nuclei) form a narrow cone centered on the beam direction (see Fig. 1). In the simple case of a single  $\gamma$  transition to the ground state, perpendicular to the beam direction ( $\theta_\gamma = \pi/2$ ), the maximum angle of the recoil nucleus can be calculated to be:

$$\theta_{r,max} \simeq \arctan \left( \frac{Q + E_{cm}}{\sqrt{2m_1 c^2 \left( \frac{m_1 + m_2}{m_2} \right) E_{cm}}} \right) \quad (2)$$

A similar relation to Eq. (2) can also be derived for the momentum spread of the recoils,  $\Delta p/p$ . The minimum of both relations appears at  $E_{cm} = Q$ . This behavior is very interesting, since in the astrophysically relevant energy region, reactions with  $Q/E_{cm} < 1$  have increasing  $\theta_{r,max}$  with increasing energy, while reactions with  $Q/E_{cm} > 1$  exhibit the opposite behavior. For example, the  ${}^7\text{Be}(p, \gamma){}^8\text{B}$  reaction, with a  $Q$  value of 136.4 keV can be a very challenging measurement for resonances with  $E_r > Q$ , since  $\theta_{r,max}$  increases with increasing energy [1]. On the other hand, for resonances with  $E_r \sim 1$  MeV, typical for astrophysical environments, the  ${}^6\text{Li}(\alpha, \gamma){}^{10}\text{B}$  ( $Q$ -value = 4461.19 keV), has a decreasing  $\theta_{r,max}$  with increasing energy, which is similar to the  ${}^7\text{Be}(\alpha, \gamma){}^{11}\text{C}$  reaction ( $Q$ -value = 7543.6 keV), and for this reason is a good choice for a surrogate reaction. For a more detailed discussion regarding the kinematics formalism of radiative capture reactions using recoil separators for astrophysics the reader is referred to Refs. [1,2].

What is really important in the case of an experimental study is not the maximum cone angle of the recoils, but rather their angular distribution, which affects the number of recoils within a given angular range of zero degrees, ultimately defining the transmission efficiency of recoils through the separator. The recoil angular distribution depends on the  $\gamma$  cascade and more specifically on the  $\gamma$  branching ratios and the  $\gamma$  angular distribution. To illustrate the above statements, we show in Fig. 2 how the recoil angular distribution of the  $E_r = 1458.5(6)$  keV resonance of  ${}^6\text{Li}(\alpha, \gamma){}^{10}\text{B}$  reaction can be affected by changing either the number of the  $\gamma$  rays in the cascade (left) or their angular distribution (right), which can be a M1/E2 decay from the  $J = 2^+$  state to the  $J = 1^+$  and  $J = 3^+$  states. It is evident that a single transition to the ground state results in a distribution with a peak closer to the maximum angle  $\theta_{r,max}$ , while multiple  $\gamma$  rays shift the distribution to smaller angles. This behavior affects both the recoil transmission through the separator and the efficiency of the  $\gamma$  ray detection system. As far as the  $\gamma$  angular correlations are concerned, for the case of radiative  $\alpha$  capture on  ${}^6\text{Li}$  in the center of mass system, the quadrupole distribution ( $W(\theta) \propto \sin^2 \theta \cos^2 \theta$ ) shifts the average recoil momentum angle to smaller angles, compared to the uniform ( $W(\theta) = 1$ ) and dipole

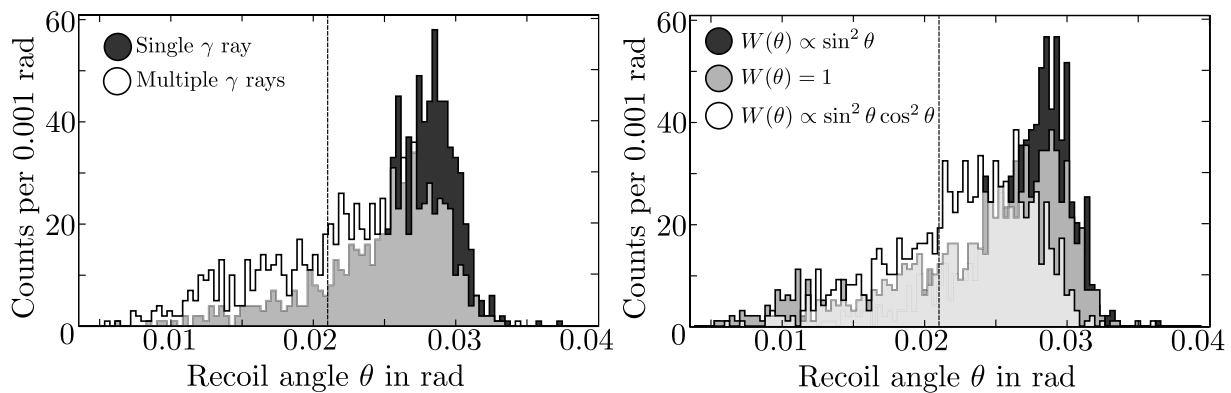


**Fig. 2.** GEANT simulation results for the recoil angular distribution of the  $E_r = 1458.5$  keV resonance of  ${}^6\text{Li}(\alpha, \gamma){}^{10}\text{B}$  reaction by changing (Left) the number of  $\gamma$  rays emitted in the cascade and (Right) their angular distribution (Dipole -  $W(\theta) \propto \sin^2 \theta$ , Uniform -  $W(\theta) = 1$  and Quadrupole -  $W(\theta) \propto \sin^2 \theta \cos^2 \theta$ ). The vertical line shows DRAGON's angular acceptance,  $\pm 21$  mrad. See the text for details.

**Table 2**

Tabulated results of the GEANT simulations presented in Fig. 2. See the text for details.

# of emitted $\gamma$ rays	$\gamma$ angular distribution, $W(\theta)$	Separator transmission (%)	BGO efficiency (%)
1	Uniform	$5.89 \pm 0.83$	$73.58 \pm 15.52$
3	Uniform	$27.4 \pm 1.9$	$80.4 \pm 7.6$
2	Uniform	$7.31 \pm 0.93$	$69.7 \pm 13.4$
2	Dipole	$11.86 \pm 1.21$	$64.81 \pm 9.95$
2	Quadrupole	$17.08 \pm 1.48$	$73.25 \pm 8.99$

( $W(\theta) \propto \sin^2 \theta$ ) cases, as we can see in Fig. 2 – Right. Table 2 shows an overview of the GEANT simulation that we discussed in the above.

Recoil separators are built with an intrinsic angular acceptance, which sets a geometric limit to the number of reactions they can study. Table 1 shows an overview of some important astrophysical reactions and their respective recoil cone angles at energies relevant for astrophysics. For some of them the maximum momentum angle of the recoils is quite large ( $>30$  mrad), posing a great challenge to study them in inverse kinematics using recoil separators. The reaction we selected to study in this work,  ${}^6\text{Li}(\alpha, \gamma){}^{10}\text{B}$ , has a maximum recoil angle of  $\theta_{r, \max} = \pm 32$  mrad at  $E_{cm} = 1458.5(6)$  keV, which is 22 mrad greater than DRAGON's angular acceptance ( $\theta_{\text{DRAGON}} = \pm 21$  mrad).

In cases like that, the planning of an experiment and the subsequent analysis relies heavily on detailed simulations of the separator (GEANT in the case of DRAGON) which provides information about the transmission of the recoils and the resonance energy. It is very useful to have a prior knowledge of the  $\gamma$  branching ratios and the  $\gamma$  angular distributions, but even in the case of a completely unknown  $\gamma$  cascade, simulations can be used to estimate the branching ratios [1].

### 3. Previous measurement

The only published measurement of  ${}^6\text{Li}(\alpha, \gamma){}^{10}\text{B}$  reaction's  $E_r = 1458.5(6)$  keV ( $E_x = 5919.5(6)$  keV) resonance strength was performed by Forsyth et al. [9]. The measurement was carried out at the University of Maryland Van de Graaff accelerator lab in regular kinematics, using a singly-charged  ${}^4\text{He}$  beam ( $E_\alpha = 0.9\text{--}3.3$  MeV &  $I_\alpha = 2.5$   $\mu\text{A}$ ) and a 96% isotopically enriched  ${}^6\text{Li}$  target.  $\gamma$  rays were detected using a NaI crystal placed at  $90^\circ$  with respect to the beam.

The resonance strength was found to be  $\omega\gamma = 0.228(38)$  eV and its width  $\Gamma = 6(1)$  keV in the center of mass system. Branching ratios of the  $\gamma$  transitions were determined to be 82(5) % and 18(5) % to the ground state and the first excited state, respectively (see Fig. 3), contrary to a single transition to the ground state reported in a study by Meyer-Schützmeister and Hanna [11]. The reported branching ratios were

used as input for the GEANT simulations of DRAGON, which provided the recoil transmission and the BGO  $\gamma$  array detection efficiency (see Section 5.5).

### 4. Experimental details

Our study was carried out in inverse kinematics using a beam of  ${}^6\text{Li}^+$  from OLIS, which was accelerated through the ISAC-I Radio-Frequency Quadrupole (RFQ) and Drift-Tube Linac (DTL) to an average energy of 0.612(1) A MeV ( $E_{lab} = 3.675(6)$  MeV,  $E_{cm} = 1.468(3)$  MeV), so that the resonance was centered in the gas target. The beam energy spread was  $\Delta E/E \leq 0.3\%$  throughout the experiment [13], with an average intensity of  $1.94 \times 10^{10} \text{ s}^{-1}$  (see also Section 5.2). The windowless gas target pressure was maintained at  $P = 5.0(1)$  Torr, corresponding to a thickness of  $1.97(4) \times 10^{18} \text{ atoms/cm}^2$ . Choosing the aforementioned beam energy and gas target pressure, we were covering a center-of-mass energy window of  $1458.5 \pm 10$  keV. The most intense charge state of the recoils ( ${}^{10}\text{B}^{2+}$ ) was tuned through the separator to a 66  $\mu\text{m}$  thick, gridded Double-Sided Silicon Strip Detector (DSSSD) placed near the focal plane of DRAGON with a typical rate of 15–20 Hz.

### 5. Data analysis & results

To extract the resonance strength and compare it to the literature value, we first had to calculate the reaction yield, which includes identifying the recoils, determining the total number of beam particles, measuring the charge-state fraction of the recoils, and calculating the efficiency of the BGO array as well as the transmission of the recoils through the separator using GEANT simulations.

#### 5.1. Particle identification

The  ${}^{10}\text{B}$  recoils were detected by the DSSSD in coincidence with  $\gamma$  rays in the BGO array. Further discrimination was provided using software cuts on the separator time-of-flight (see Fig. 6), which is defined as the time difference between a  $\gamma$  hit in a BGO detector and a hit in the DSSSD at the focal plane of DRAGON [14]. DRAGON is very efficient in rejecting unreacted beam ions for ( $\alpha, \gamma$ ) reactions, with demonstrated suppression factors of  $> 10^{13}$ , which can be increased by few orders of magnitude, by using the aforementioned software cuts [1,5,15].

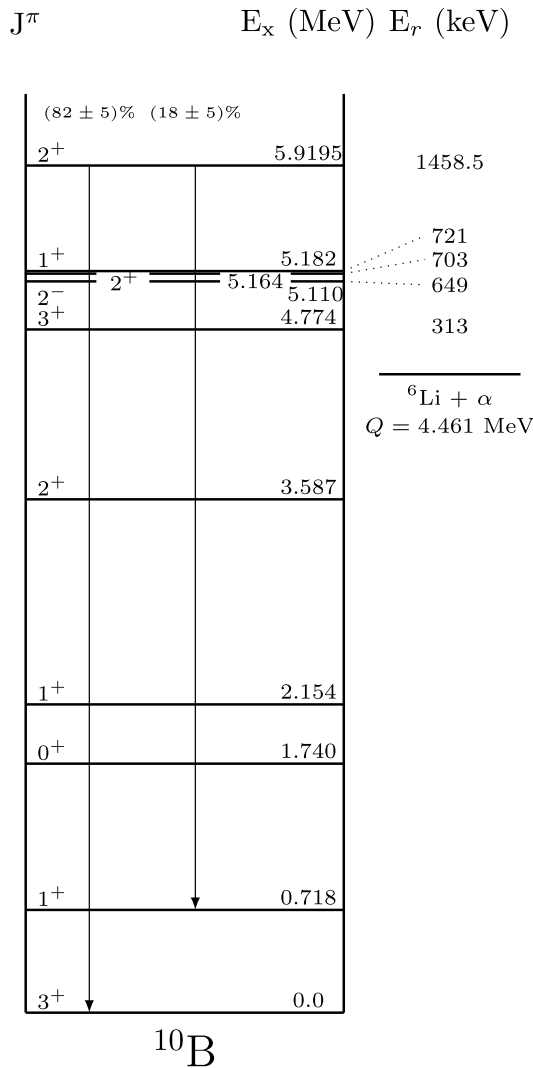


Fig. 3. Partial level scheme of the low-lying energy levels of  $^{10}\text{B}$ . Two  $\gamma$ -transitions of the  $E_x = 5919.5(6)$  keV state are shown. The reaction  $Q$  value was taken from AME2016 [12].

### 5.2. Beam normalization

To ensure a precise measurement of the reaction yield, we monitored the beam current throughout the experiment using Faraday cups located along DRAGON. In particular, the number of beam ions  $N_{beam}$ , impinging on the windowless gas target is calculated using the following method: a silicon surface barrier (SSB) detector placed at a well-defined lab angle of  $57^\circ$  inside the target was detecting the elastically scattered gas target particles during each run. For a time window  $\Delta t \sim 240$  s, before and after each run, we recorded these measurements. At the same time, beam current measurements were made at a Faraday cup located 2 m upstream of the target. The normalized number of beam ions,  $N_{beam}$ , is then given by:

$$N_{beam} = \mathcal{R} N_\alpha \frac{E^2}{P} \quad (3)$$

where  $E$  is the beam energy and  $P$  is the gas target pressure.  $\mathcal{R}$  is the normalization coefficient, given by:

$$\mathcal{R} = \frac{I}{|e|} \frac{\Delta t}{N_\alpha} \frac{P}{E^2} \eta_{trg} \quad (4)$$

where  $I/|e|$  is the current reading at the aforementioned Faraday Cup in ions per second,  $\eta_{trg}$  is the beam transmission through an empty

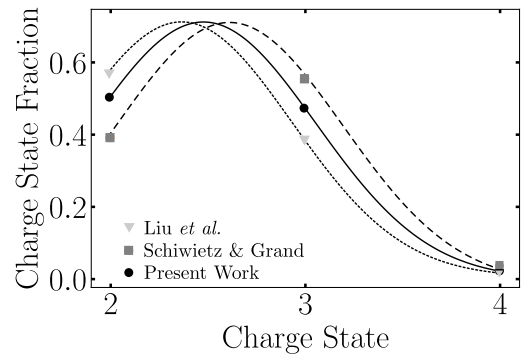


Fig. 4. Comparison between the experimentally measured CSD ( $\eta_{CSD}$ ) for  $^{11}\text{B}$  with the semi-empirical formulae of Liu et al. [16] and Schiwietz & Grand [17]. The fit to the experimental data is a Gaussian function. The error bars are smaller than the size of the points.

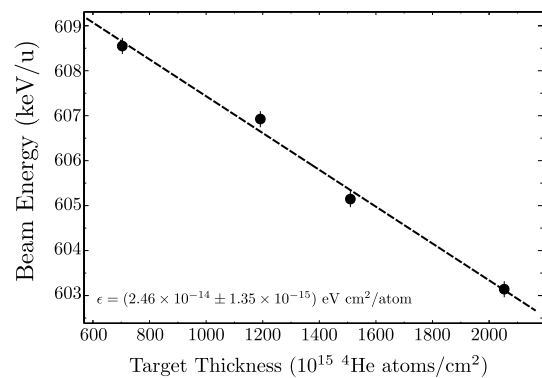


Fig. 5. Gas target thickness versus beam energy for different values of the target pressure. The slope of the linear fit is the stopping power  $\epsilon$ .

target,  $q$  is the charge state of the beam ( $1^+$ ), and  $N_\alpha$  is the number of scattered target ( $\alpha$ ) nuclei into the surface barrier detector during  $\Delta t$ .

### 5.3. Boron charge state distribution

Given that DRAGON is tuned to select and transport only a single recoil charge state to the final focal plane, it is necessary to measure the recoil charge state distribution (CSD) using a beam of an abundant isotope of the recoil element, to determine the total reaction yield. Charge State Distribution measurements were performed using a  $^{11}\text{B}$  beam provided by OLIS. The results are compared with the semi-empirical formulae of Liu et al. [16] and Schiwietz & Grand [17] (see Fig. 4).

### 5.4. $^6\text{Li}$ stopping power in $^4\text{He}$

One of the advantages of studying reactions using recoil separators is that the stopping power  $\epsilon$ , which is required for the calculation of the resonance strength, is measured directly and is not based on semi-empirical formulae, which introduce an additional uncertainty to the measurement, especially when they are extrapolated to low energies. At DRAGON, stopping powers are measured by varying both the pressure in the gas target and the magnetic field strength needed to center the beam at a momentum dispersed angular focus in the focal plane of the first magnetic dipole of DRAGON (see Fig. 5). We used these results to calculate the expected yield  $Y_{\omega\gamma_0}$  in Eq. (5) and compare our experimental results with GEANT simulations (see Section 5.5).

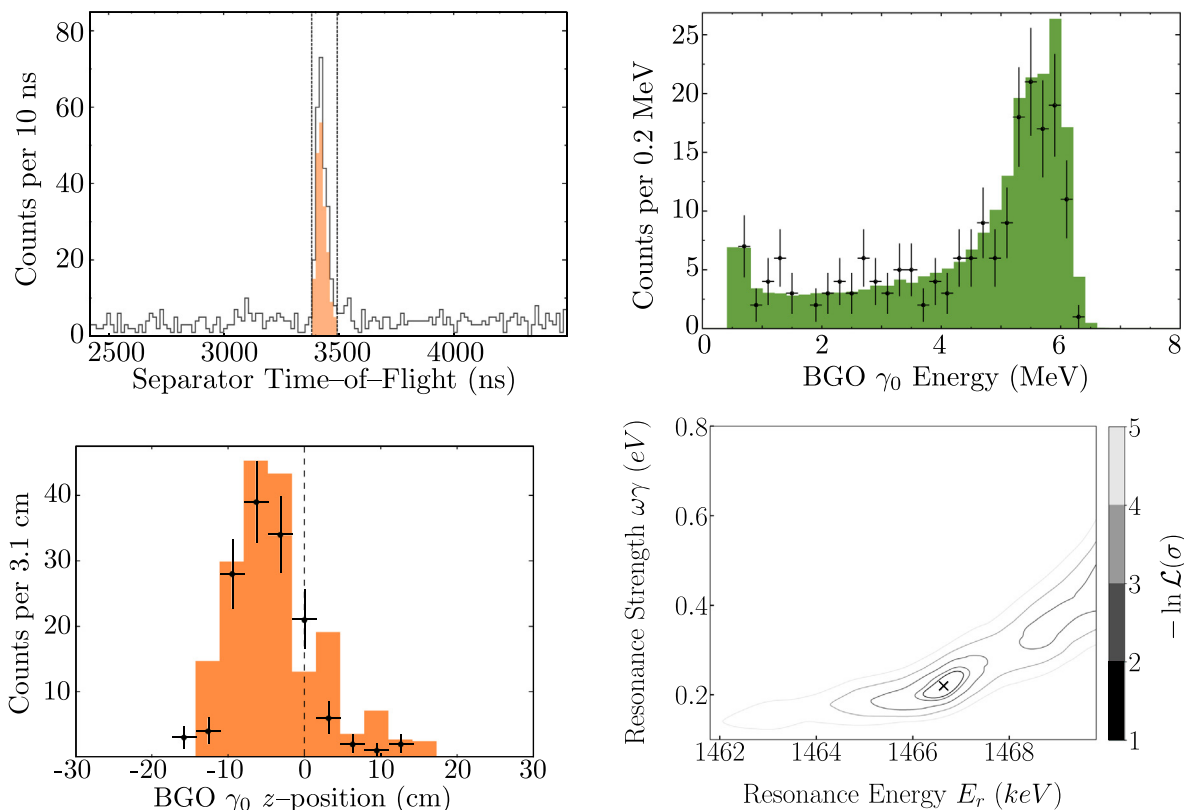


**Fig. 6.** (Top Left) Separator time-of-flight spectrum for particle identification. The gate shown is for  $\tau = 3.38 - 3.49 \mu\text{s}$ . (Top Right)  $\gamma_0$  energy plot comparison between experiment (black points) and GEANT simulation (green histogram). Both transitions of the  $E_r = 1458.5 \text{ keV}$  resonance can be seen. (Bottom Left) The distribution of the  $z$ -position of the highest energy  $\gamma$  ray for a yield measurement at  $P = 5 \text{ Torr}$ . The centroid is at  $-3.85 \text{ cm}$  from the center of the gas target. The orange histogram shows the global best fit by means of GEANT simulations (Bottom Right) Negative Log-likelihood contour plot for the  $(E_r, \omega\gamma)$  space. The gray cross shows the minimum. See the text for a detailed discussion. (For interpretation of the references to color in this figure legend, the reader is referred to the web version of this article.)

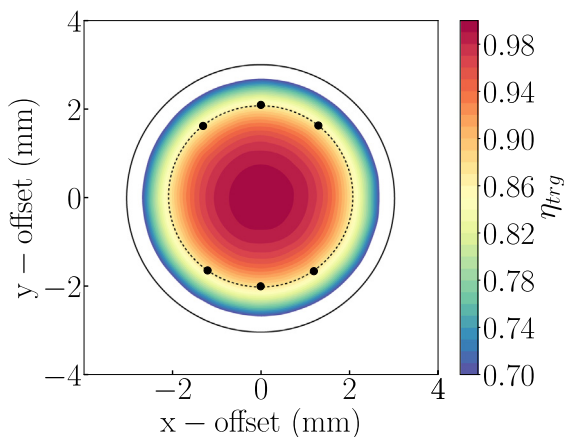


**Fig. 7.** (Color online) Beam transmission results for a beam with  $2 \times \text{rms}$  size of  $1.78 \text{ mm}$  in  $x$ - and  $y$ -axis. The black points show the locations selected for additional GEANT simulations. See the text for details.

### 5.5. Log-likelihood analysis for $E_r$ & $\omega\gamma$

The analysis of the BGO detector spectrum for the highest energy  $\gamma$  ray emitted by the de-excitation of the  $^{10}\text{B}$  recoils (Fig. 6) shows that the resonance is excited upstream of the center of the gas target, indicating that the resonance energy is higher than  $1458.5 \text{ keV}$ . Therefore, we cannot use the standard method of DRAGON to determine the resonance energy from the distribution of the  $z$  position of the highest energy  $\gamma$  ray, since it assumes that the resonance is excited in the uniform density region surrounding the center of the gas target [18].

Instead, we performed a likelihood analysis similar to the ones in Refs. [19,20] to extract the resonance energy  $E_r$ , and its strength  $\omega\gamma$ .

To begin, we performed simulations for the  $z$  distribution of the highest energy  $\gamma$  rays using different resonance energies (13 values, spanning from  $E_r = 1457.8$  to  $1469.8 \text{ keV}$ ) and a fixed beam energy of  $3.675 \text{ MeV}$  and spread equal to the experimental one, with the standard DRAGON GEANT3 simulation package<sup>1</sup> [21]. The GEANT input file included nuclear level information, such as lifetimes and  $\gamma$  branching ratios, from Ref. [22] (see Table 3). For the  $\gamma$  ray angular distribution, which as we discussed earlier affects the recoil transmission through the separator, we proceeded as follows: a spin 1 beam ( $^6\text{Li}$ ) on a spin 0 target ( $^4\text{He}$ ) can populate  $M = 0, \pm 1$  magnetic substates of  $^{10}\text{B}$ . Using Ref. [23], we found the statistical tensor coefficients  $\rho_2(2, 0) = \rho_2(2, 1) = -1.195$ . Then we multiplied with the geometry factors  $R_2(2 \rightarrow 3) = 0.1195$  and  $R_2(2 \rightarrow 1) = 0.4183$ , which results in the  $\gamma$  angular distribution for the two transitions:  $W(\theta) = 0.86 + 0.21 \sin^2(\theta)$  to the  $J = 3$  ground state and  $W(\theta) = 0.5 + 0.75 \sin^2(\theta)$  to the  $J = 1$  first excited state. Therefore the angular distribution of the dominant ground state transition is nearly isotropic and that of the other is between isotropic and bipolar.

In addition, we took into account the transmission of the beam through the gas target. In particular, during the experiment we measured an  $\sim 86\%$  transmission of the beam through the gas target by means of Faraday cup measurements. This implies that the beam was not centered as it was entering the gas target, given that its  $2 \times \text{rms}$  size, assuming a Gaussian profile, was measured by the ISAC operators to be  $1.78 \text{ mm}$  in both  $x$  and  $y$ . To include this piece of information in our GEANT simulations, we performed Monte-Carlo simulations sampling

<sup>1</sup> The GEANT3 simulation package of DRAGON can be found at [https://github.com/DRAGON-Collaboration/G3\\_DRAGON](https://github.com/DRAGON-Collaboration/G3_DRAGON).

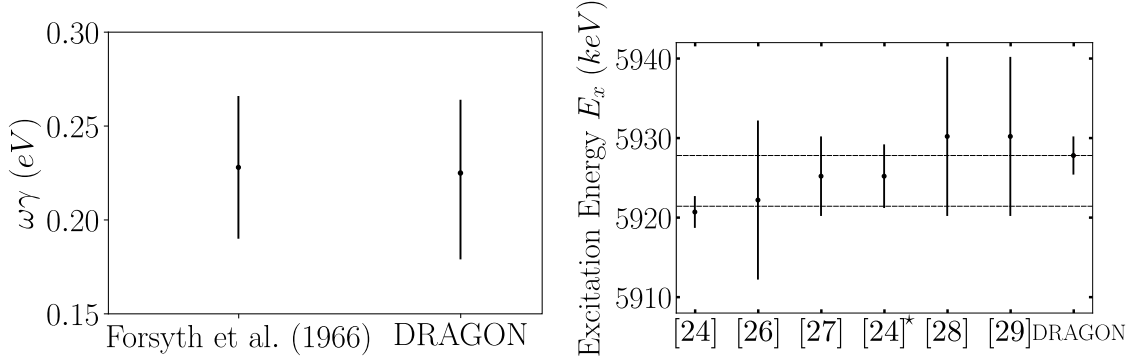


**Fig. 8.** (Left) Comparison between the result of Forsyth et al. and the present work for the resonance strength of the  $E_r = 1458.5$  keV resonance. (Right) Excitation energies for the  $E_x = 5919.5$  keV state of  $^{10}\text{B}$  from normalized literature values (Table 6) compared with the present work. The band correspond to the EVM average uncertainty. See the text for a detailed discussion.

**Table 3**

Settings of the GEANT3 simulation for the Log-Likelihood analysis. Nuclear properties were adopted from Ref. [22]. See the text for details.

Quantity	Used Value
Excited state lifetime	$1.13 \times 10^{-19}$ s
Resonance energy	1457.8–1469.8 keV
Beam mass excess	14.087 MeV
Recoil mass excess	12.051 MeV
$\alpha$ partial width	5.82 keV
$\gamma$ partial width	0.1114 eV
$\gamma$ branching ratios	82% (to the ground state) 18% (to the first excited)
$\gamma$ angular distributions	
$2 \rightarrow 3$ (ground state)	$W(\theta) = 0.86 + 0.21 \sin^2(\theta)$
$2 \rightarrow 1$ (first excited)	$W(\theta) = 0.50 + 0.75 \sin^2(\theta)$

both x- and y-axis offsets for the measured beam size. Fig. 7 shows the results of the simulated transmission. After that, we selected six point with 86% transmission to perform our simulations (black points in Fig. 7).

We then scaled the generated BGO spectra according to the expected reaction yield by a factor

$$\eta \frac{Y_{\omega\gamma_0} N_{beam}}{N_{sim}}, \quad (5)$$

where  $\eta$  is the recoil detection efficiency,<sup>2</sup>  $Y_{\omega\gamma_0}$  is the reaction yield from a single-level Breit-Wigner resonance ( $\Gamma = 5.82$  keV [22]) of arbitrary strength  $\omega\gamma$  (200 values spanning from 0.05–10 eV),  $N_{beam}$  is the number of incident beam ions (See Section 5.2) and  $N_{sim} = 5 \times 10^4$  is the number of simulated events. The BGO array  $\gamma$  ray detection efficiency  $\eta_{BGO}$  and the separator transmission  $\eta_{separator}$  are built-in the GEANT simulation, and thus we do not include them in the  $\eta$  factor. The simulated  $\gamma$  spectra are convoluted with a Gaussian resolution function with  $\sigma(E) = 0.1733\sqrt{E}/(\ln 2\sqrt{8})$ , which is based on the experimentally measured resolution of the BGO array. The scaled BGO spectra are then compared to the experimental data. From these simulations we created a  $(E_r, \omega\gamma)$  space of 2600 points ( $13 \times 200$ ) and for each point on this grid, we calculated the negative log-likelihood using:

$$-\ln \mathcal{L} = \sum_i [\ln(n_i!) - n_i \ln(f_i)] + S, \quad (6)$$

where  $i$  is the number of bins in the experimental BGO spectrum,  $n_i$  is the number of events in the  $i$ th bin,  $f_i$  is the number of events in the scaled simulation  $i$ th bin and  $S$  the total number of events in the scaled histogram.

Fig. 6 shows the results of our simulations with a single minimum for the negative log-likelihood, with energy that corresponds to a

<sup>2</sup> It includes the recoil charge state fraction, the heavy ion detector efficiency, and the data acquisition dead time.

**Table 4**

Relative systematic uncertainties used to calculate the resonance strength of the  $E_r = 1458.5$  keV resonance.

Quantity	Measured Value	Relative Uncertainty
$\eta_{CSF}$	0.523(8)	1.5%
$N_{beam}$	$3.252(53) \times 10^{14}$	1.64%
$\eta_{BGO}$	0.332(38)	11.4%
$\eta_{separator}$	0.122(5)	4.1%
$\epsilon$ (eV cm <sup>2</sup> )	$24.63(136) \times 10^{15}$	5.5%
$\eta_{lifetime}$	0.91573(8)	0.009%
$E_{beam}$ (A MeV)	0.612(1)	0.16%
<b>Total systematic uncertainty</b>		<b>13.49%</b>

location inside the gas target. The global minimum has  $-\ln \mathcal{L}_0 = 35.69$  and it is the only point where a  $1\sigma$  contour can be deduced.

On top of the above analysis, we also performed tests on the GEANT simulation by changing the random seed of the Monte Carlo simulation, to ensure that the distribution of events is Poissonian, as in an experimental study. Due to the large number of simulation events ( $N_{sim} = 5 \times 10^4$ ) the final result does not depend on the random seed.

The sources of systematic uncertainty in the final result for the resonance strength are presented in Table 4. The most important source of systematic uncertainty is the BGO efficiency which accounts for 11.4% and it was determined by varying the  $\gamma$  branching ratios of the resonance. The statistical uncertainty originates from the Log-Likelihood analysis and is defined by the bounds of the  $1\sigma$  contour ( $\delta\omega\gamma = {}^{+0.025}_{-0.035}$  eV) For the level excitation energy,  $E_x$ , we have similarly taken into account the statistical uncertainty from the Log-Likelihood analysis,  $\pm 0.5$  keV, and for the systematic uncertainty, we adopt the relative uncertainty of the beam energy  $\delta E_{beam} = 0.16\%$ , which yields  $\delta E_x(\text{syst.}) = 2.4$  keV.

The results for the resonance energy  $E_r$ , excitation energy  $E_x$  and strength  $\omega\gamma$ , for this minimum are the following:

$$E_r = 1466.6 \pm 0.5 \text{ (stat.)} \pm 2.4 \text{ (syst.) keV}$$

$$E_x = 5927.8 \pm 0.5 \text{ (stat.)} \pm 2.4 \text{ (syst.) keV}$$

$$\omega\gamma = 0.225 {}^{+0.025}_{-0.035} \text{ (stat.)} \pm 0.030 \text{ (syst.) eV}$$

Our final resonance strength is in excellent agreement with the measurement of Forsyth et al. [9] as shown in Fig. 8. However, the resonance energy (excitation energy) we extracted with DRAGON is higher than the recommended value in nuclear databases [24]. A literature search (Refs. [25–29,29,30]) shows that the excitation energy  $E_x$ , for the state of interest lies between 5920–5930 keV, which is consistent with our result (see Table 6 and Fig. 8). To obtain an average literature-based excitation energy with a realistic uncertainty, we first excluded the measurement of Buccino & Smith [26] as an outlier ( $E_x = 5900 \pm 80$  keV) applying Peirce's criterion [31]. We then

**Table 5**  
Evolution of the  ${}^6\text{Li}(\alpha, \gamma){}^{10}\text{B}$  reaction  $Q$  value through the years. See the text for details.

Year	$Q$ value (keV)	$\Delta Q$ (keV)	Ref.
2017	4461.19	–	[12]
2004	4461.10	+0.09	[22]
1988	4459.60	+1.59	[39]
1984	4460.30	+0.89	[38]
1979	4460.50	+0.69	[37]
1974	4460.00	+1.19	[36]
1966	4461.00	+0.19	[35]
1959	4459.00	+2.19	[34]

**Table 6**  
Summary of reported energies for the  $E_x = 5920$  keV state of  ${}^{10}\text{B}$  from different measurements, normalized to the current  ${}^6\text{Li}(\alpha, \gamma){}^{10}\text{B}$  reaction  $Q$  value [12]. See the text for a detailed discussion.

Reaction	$E_x$ (keV)	$\delta E_x$ (keV)	Reference
${}^9\text{Be}(d, n){}^{10}\text{B}$	5902.2	80	Buccino & Smith [26]
${}^{10}\text{B}(p, p'){}^{10}\text{B}$	5920.7	0.6	Kashy, Benenson & Nolen Jr. [25]
${}^{10}\text{B}(d, d'){}^{10}\text{B}$	5922.2	10	Armitage & Meads [27]
${}^{10}\text{B}(p, p'){}^{10}\text{B}$	5922.2	10	Armitage & Meads [27]
${}^{11}\text{B}({}^3\text{He}, \alpha){}^{10}\text{B}$	5925.2	5	Gorodetsky et al. [28]
N/A	5925.2	4	Reported in Ref. [25]
${}^9\text{Be}(d, n){}^{10}\text{B}$	5930.2	10	Park et al. [29]
${}^9\text{Be}(d, n){}^{10}\text{B}$	5930.2	10	Fife et al. [30]
<b>Average</b>	5921.3	3.2	Without normalized $Q$ value
<b>Average</b>	5924.6	3.2	With normalized $Q$ value
<b><math>{}^6\text{Li}(\alpha, \gamma){}^{10}\text{B}</math></b>	5927.8	$\pm 0.5$ (stat.) $\pm 2.4$ (syst.)	DRAGON

calculated the average using the Expected Value Method (EVM) [32] for all the remaining measurements with reported uncertainties to be  $E_x = (5920.3 \pm 2.4)$  keV. It is worth mentioning that the adopted level energy of  $E_x = (5919.5 \pm 0.6)$  keV [24] is mainly determined by the high-precision measurement reported in Ref. [25]. However, this result was extracted using an Enge split-pole spectrograph which usually results in excitation energy uncertainties of approximately  $\pm 5$  keV [33]. For this reason, we also calculated the EVM average with a more realistic uncertainty for the study of Ref. [25], based on their analysis –  $\delta E_x = 2$  keV – to be  $E_x = (5921.2 \pm 3.2)$  keV. Furthermore, we investigated how the reaction  $Q$  value changed between the literature measurements. We found a  $\sim 1 - 2$  keV difference between the  $A = 10$  evaluations and the AME2016 compilation, which we used for our calculations [12, 22, 34–39] (see also Table 5). In particular, the  $Q$  value changes between the 1979 to 1984 and 1984 to 1988 evaluations are based on mass measurements reported in Refs. [40] and [41], respectively. For this reason, we adjusted the literature values of the excitation energy to the current  $Q$  value, assuming that they were following the latest  $A = 10$  evaluation at the time of publication (see Table 6). The new result,  $E_x = (5924.6 \pm 3.2)$  keV agrees within  $1\sigma$  with the energy extracted using the Negative Log-Likelihood analysis  $E_x = 5927.8 \pm 0.5$  (stat.)  $\pm 2.4$  (syst.) keV (see Fig. 8).

## 6. Discussion & conclusions

As this work demonstrates, such measurements can provide a test of the limits of the DRAGON angular acceptance, using a known resonance of the  ${}^6\text{Li}(\alpha, \gamma){}^{10}\text{B}$  reaction. It is worth noting that such measurements can provide reliable results only if they are coupled with detailed simulations of the separator, which provide the important information on the recoil transmission and the  $\gamma$  ray detection efficiency. The data analysis is also affected by our knowledge of the  $\gamma$  branching ratios and angular distributions  $W(\theta)$ , as discussed in Section 2. Accurate measurements of the  $\gamma$  branching ratios using high efficiency detectors are desirable, but even if they are unknown, the  $\gamma$  ray detection efficiency can still be calculated using a combination of the experimental data and simulations [1]. The final result, however, might suffer from higher systematic uncertainty.

The results we obtained in this work are in excellent agreement with the only known measurement by Forsyth et al. showing that DRAGON can measure resonance strengths of reactions with large recoil angular cones. We can now proceed with confidence to study a wide range of alpha-capture reactions (see Table 1), previously thought inaccessible with DRAGON due to recoil acceptance constraints. This includes a planned measurement of the  ${}^7\text{Be}(\alpha, \gamma){}^{11}\text{C}$  reaction at energies relevant to  $\nu p$ -process nucleosynthesis.

## CRedit authorship contribution statement

**A. Psaltis:** Software, Validation, Formal analysis, Investigation, Data curation, Writing - original draft, Writing - review & editing, Visualization. **A.A. Chen:** Conceptualization, Investigation, Resources, Writing - review & editing, Supervision, Funding acquisition. **D.S. Connolly:** Software, Investigation. **B. Davids:** investigation, Writing - review & editing. **G. Gilardy:** Investigation. **R. Giri:** Investigation. **U. Greife:** Investigation. **W. Huang:** Investigation. **D.A. Hutcheon:** Investigation, Resources, Writing - review & editing. **J. Karpesky:** Investigation. **A. Lennarz:** Investigation, Writing - review & editing. **J. Liang:** Investigation. **M. Lovely:** Investigation. **S.N. Paneru:** Investigation. **C. Ruiz:** Conceptualization, Methodology, Investigation, Resources, Writing - review & editing, Project administration, Funding acquisition. **G. Tenkila:** Investigation. **M. Williams:** Investigation, Writing - review & editing.

## Declaration of competing interest

The authors declare that they have no known competing financial interests or personal relationships that could have appeared to influence the work reported in this paper.

## Acknowledgments

The authors gratefully acknowledge the beam delivery and ISAC operations groups at TRIUMF. The core operations of TRIUMF are supported via a contribution from the federal government through the National Research Council of Canada, and the Government of British Columbia provides building capital funds. DRAGON and authors from McMaster University are receive funds from the National Sciences and Engineering Research Council of Canada (NSERC). A.P. thanks Greg Christian (St. Mary's University) for valuable discussions concerning the GEANT simulations, and the anonymous reviewers whose comments/suggestions helped improve and clarify this manuscript. Authors from the UK are supported by the Science and Technology Facilities Council. Authors from Colorado School of Mines acknowledge support from U.S. Department of Energy Office of Science DE-FG02-93ER40789 grant. This work benefited from discussions at the ‘‘Nuclear Astrophysics at Rings and Recoil Separators’’ Workshop supported by the National Science Foundation under Grant No. PHY-1430152 (JINA Center for the Evolution of the Elements).

## References

- [1] C. Ruiz, U. Greife, U. Hager, Recoil separators for radiative capture using radioactive ion beams, *Eur. Phys. J. A* 50 (6) (2014) 99.
- [2] C.R. Brune, B. Davids, Radiative capture reactions in astrophysics, *Annu. Rev. Nucl. Part. Sci.* 65 (2015) 87–112.
- [3] D. Hutcheon, S. Bishop, L. Buchmann, M. Chatterjee, A. Chen, J. D'Auria, S. Engel, D. Gliotti, U. Greife, D. Hunter, et al., The DRAGON facility for nuclear astrophysics at TRIUMF-ISAC: design, construction and operation, *Nucl. Instrum. Methods Phys. Res. A* 498 (1–3) (2003) 190–210.
- [4] C. Vockenhuber, L. Buchmann, J. Caggiano, A. Chen, J. D'Auria, C. Davis, U. Greife, A. Hussein, D. Hutcheon, D. Otte, et al., Improvements of the DRAGON recoil separator at ISAC, *Nucl. Instrum. Methods Phys. Res. B* 266 (19–20) (2008) 4167–4170.
- [5] S. Sjuve, B.N. Singh, P. Adsley, L. Buchmann, M. Carmona-Gallardo, B. Davids, J. Fallis, B. Fulton, N. Galinski, U. Hager, et al., Beam suppression of the DRAGON recoil separator for  ${}^3\text{He}(\alpha, \gamma){}^7\text{Be}$ , *Nucl. Instrum. Methods Phys. Res. A* 700 (2013) 179–181.

- [6] J. Fallis, C. Akers, A. Laird, A. Simon, A. Spyrou, G. Christian, D. Connolly, U. Hager, D. Hutcheon, A. Lennarz, et al., First measurement in the Gamow window of a reaction for the  $\gamma$ -process in inverse kinematics:  $^{76}\text{Se}(\alpha, \gamma)^{80}\text{Kr}$ , *Phys. Lett. B* 807 (2020) 135575.
- [7] D. Lehbertz, S. Courtin, F. Haas, D. Jenkins, C. Simenel, M.-D. Salsac, D. Hutcheon, C. Beck, J. Cseh, J. Darai, et al.,  $^{12}\text{C}(^{16}\text{O}, \gamma)^{28}\text{Si}$  radiative capture: Structural and statistical aspects of the  $\gamma$  decay, *Phys. Rev. C* 85 (3) (2012) 034333.
- [8] C. Matei, L. Buchmann, W. Hannes, D. Hutcheon, C. Ruiz, C. Brune, J. Caggiano, A. Chen, J. D'Auria, A. Laird, et al., Measurement of the cascade transition via the first excited state of  $^{16}\text{O}$  in the  $^{12}\text{C}(\alpha, \gamma)^{16}\text{O}$  reaction, and its S factor in stellar helium burning, *Phys. Rev. Lett.* 97 (24) (2006) 242503.
- [9] P. Forsyth, H. Tu, W. Hornyak, The  $^6\text{Li}(\alpha, \gamma)^{10}\text{B}$  reaction and the energy levels of  $^{10}\text{B}$ , *Nucl. Phys.* 82 (1) (1966) 33–48.
- [10] K. Jayamanna, F. Ames, G. Cojocaru, R. Baartman, P. Bricault, R. Dube, R. Laxdal, M. Marchetto, M. MacDonald, P. Schmor, et al., Off-line ion source terminal for ISAC at TRIUMF, *Rev. Sci. Instrum.* 79 (2) (2008) 02C711.
- [11] L. Meyer-Schützmeister, S. Hanna, Energy levels in  $^{10}\text{B}$  in the reaction  $^6\text{Li}(\alpha, \gamma)^{10}\text{B}$ , *Phys. Rev.* 108 (6) (1957) 1506.
- [12] M. Wang, G. Audi, F. Kondev, W. Huang, S. Naimi, X. Xu, The AME2016 atomic mass evaluation (II). Tables, graphs and references, *Chin. Phys. C* 41 (3) (2017) 030003.
- [13] R. Laxdal, Acceleration of radioactive ions, *Nucl. Instrum. Methods Phys. Res. B* 204 (2003) 400–409.
- [14] G. Christian, C. Akers, D. Connolly, J. Fallis, D. Hutcheon, K. Olchanski, C. Ruiz, Design and commissioning of a timestamp-based data acquisition system for the DRAGON recoil mass separator, *Eur. Phys. J. A* 50 (4) (2014) 75.
- [15] D. Hutcheon, L. Buchmann, A. Chen, J. D'Auria, C. Davis, U. Greife, A. Hussein, D. Ottewell, C. Ouellet, A. Parikh, et al., Background suppression by the DRAGON radiative capture facility at TRIUMF/ISAC, *Nucl. Instrum. Methods Phys. Res. B* 266 (19–20) (2008) 4171–4175.
- [16] W. Liu, G. Imbriani, L. Buchmann, A. Chen, J. D'Auria, A. D'Onofrio, S. Engel, L. Gialanella, U. Greife, D. Hunter, et al., Charge state studies of low energy heavy ions passing through hydrogen and helium gas, *Nucl. Instrum. Methods Phys. Res. A* 496 (1) (2003) 198–214.
- [17] G. Schiwietz, P. Grande, Improved charge-state formulas, *Nucl. Instrum. Methods Phys. Res. B* 175 (2001) 125–131.
- [18] D. Hutcheon, C. Ruiz, J. Fallis, J. D'Auria, B. Davids, U. Hager, L. Martin, D. Ottewell, S. Reeve, A. Rojas, Measurement of radiative capture resonance energies with an extended gas target, *Nucl. Instrum. Methods Phys. Res. A* 689 (2012) 70–74.
- [19] L. Erikson, C. Ruiz, F. Ames, P. Bricault, L. Buchmann, A. Chen, J. Chen, H. Dare, B. Davids, C. Davis, et al., First direct measurement of the  $^{23}\text{Mg}(p, \gamma)^{24}\text{Al}$  reaction, *Phys. Rev. C* 81 (4) (2010) 045808.
- [20] G. Christian, G. Lotay, C. Ruiz, C. Akers, D. Burke, W. Catford, A. Chen, D. Connolly, B. Davids, J. Fallis, et al., Direct measurement of astrophysically important resonances in  $^{38}\text{K}(p, \gamma)^{39}\text{Ca}$ , *Phys. Rev. C* 97 (2) (2018) 025802.
- [21] D.G. Gliotti, Efficiency Calibration Measurement and GEANT Simulation of the DRAGON BGO Gamma Array at TRIUMF (Master's thesis), University of Northern British Columbia, Prince George, Canada, 2004.
- [22] D. Tilley, J. Kelley, J. Godwin, D. Millener, J. Purcell, C. Sheu, H. Weller, Energy levels of light nuclei  $A = 8, 9, 10$ , *Nuclear Phys. A* 745 (3–4) (2004) 155–362.
- [23] H. Rose, D. Brink, Angular distributions of gamma rays in terms of phase-defined reduced matrix elements, *Rev. Modern Phys.* 39 (2) (1967) 306.
- [24] NuDat, 2.8 database, in: National Nuclear Data Center, Brookhaven National Laboratory, 2020, <http://www.nndc.bnl.gov/nudat2/>.
- [25] E. Kashy, W. Benenson, J. Nolen Jr.,  $A = 9$  isospin quartet, *Phys. Rev. C* 9 (6) (1974) 2102.
- [26] S. Buccino, A. Smith, Levels in  $^{10}\text{B}$  excited by the  $^9\text{Be}(d, n)$  reaction, *Phys. Lett. (Netherlands)* 19 (1965).
- [27] B. Armitage, R. Meads, Levels in  $^{10}\text{B}$  above 5.16 MeV observed by proton and deuteron inelastic scattering, *Phys. Lett.* 8 (5) (1964) 346–349.
- [28] S. Gorodetzky, A. Gallmann, R. Rebmeister, Study of the excited states of  $^{10}\text{B}$  from 5 to 8 MeV by the  $^{11}\text{B}(^3\text{He}, \alpha)^{10}\text{B}$  reaction and a note on the  $^{11}\text{B}(^3\text{He}, t)^{11}\text{C}$  reaction, *Phys. Rev.* 137 (6B) (1965) B1466.
- [29] Y.S. Park, A. Niiler, R. Lindgren, Spectroscopy of  $^{10}\text{B}$  levels from the  $^9\text{Be}(d, n)^{10}\text{B}$  reaction, *Phys. Rev. C* 8 (5) (1973) 1557.
- [30] A. Fife, G. Neilson, W. Dawson, The excited states of  $^{10}\text{B}$ , *Nuclear Phys. A* 91 (1) (1967) 164–176.
- [31] B. Peirce, Criterion for the rejection of doubtful observations, *Astron. J.* 2 (1852) 161–163.
- [32] M. Birch, B. Singh, Method of best representation for averages in data evaluation, *Nucl. Data Sheets* 120 (2014) 106–108.
- [33] C. Marshall, K. Setoodehnia, K. Kowal, F. Portillo, A.E. Champagne, S. Hale, A. Dummer, R. Longland, The focal-plane detector package on the TUNL split-pole spectrograph, *IEEE Trans. Instrum. Meas.* 68 (2) (2018) 533–546.
- [34] F. Ajzenberg-Selove, T. Lauritsen, Energy levels of light nuclei. VI, *Nucl. Phys.* 11 (1959) 1.
- [35] T. Lauritsen, F. Ajzenberg-Selove, Energy levels of light nuclei (VII).  $A = 5-10$ , *Nucl. Phys.* 78 (1) (1966) 1–176.
- [36] F. Ajzenberg-Selove, T. Lauritsen, Energy levels of light nuclei  $A = 5-10$ , *Nuclear Phys. A* 227 (1) (1974) 1–243.
- [37] F. Ajzenberg-Selove, Energy levels of light nuclei  $A = 5-10$ , *Nuclear Phys. A* 320 (1) (1979) 1–224.
- [38] F. Ajzenberg-Selove, Energy levels of light nuclei  $A = 5-10$ , *Nuclear Phys. A* 413 (1) (1984) 1–168.
- [39] F. Ajzenberg-Selove, Energy levels of light nuclei  $A = 5-10$ , *Nuclear Phys. A* 490 (1) (1988) 1–225.
- [40] A. Chalupka, H. Vonach, E. Hueges, H. Scheerer, Precision measurement of the mass of  $^{10}\text{B}$ , *Z. Phys. A* 310 (1–2) (1983) 135–136.
- [41] R. Ellis, K. Sharma, R. Barber, S. Loewen, H. Duckworth, The precise atomic masses of  $^{10}\text{B}$  and  $^{11}\text{B}$ , *Phys. Lett. B* 141 (5–6) (1984) 306–308.